ISSN 0023-1584, Kinetics and Catalysis, 2012, Vol. 53, No. 2, pp. 239–246. © Pleiades Publishing, Ltd., 2012.

Effect of Oxygen Mobility in the Lattice of Au/TiO_2 On Formaldehyde Oxidation[1]

Dennis Y. C. Leung[a], Fu Xianliang[a], Ye Daiqi[b], and Huang Haibao[a, *]

[a] *Department of Mechanical Engineering, The University of Hong Kong*

[b] *College of Environmental Science and Engineering, South China University of Technology, China*

**e-mail: harbor@hku.hk*

Received March 01, 2011

Abstract—Two Au catalysts supported on TiO_2 were prepared by impregnation method followed by sodium borohydride reduction or calcination in air (Au/TiO_2-R and Au/TiO_2-C, respectively). The 1 wt % Au/TiO_2-R sample was found to be highly efficient for the oxidation of low concentrated formaldehyde at room temperature. A HCHO conversion of 98.5% was achieved with this catalyst, whereas the Au/TiO_2-C sample showed almost no activity under the same conditions. Highly dispersed metallic Au nanoparticles with small size (~3.5 nm) were identified in the 1 wt % Au/TiO_2-R catalyst. A significant negative shift of Au4*f* peak in XPS spectra with respect to bulk metallic Au was observed for the 1 wt % Au/TiO_2-R but no similar phenomena was found for the heat-treated catalyst. More Au nanoparticles and higher content of surface active oxygen were identified on the surface of the Au/TiO_2-R in comparison with the Au/TiO_2-C, suggesting that the Au/TiO_2-R catalyst can enhance the amount of active sites and species involved in for HCHO oxidation. The reduction treatment by sodium borohydride promotes the formation of dispersed metallic Au nanoparticles with small size because it facilitates the electron transfer and increases the content of surface Au nanoparticles and activated oxygen. All these factors are responsible for a high activity of this catalyst in the oxidation of HCHO.

DOI: 10.1134/S0023158412020048

The interest to supported gold nanoparticles was generated by the work by Haruta et al. [1] who first described an extraordinary activity of supported gold nanoparticles for low-temperature oxidation of CO was. Supported nanometer Au catalysts have been proven to be active for CO oxidation at low temperature [2–4], reduction of NO [5, 6], selective oxidation of CO in a hydrogen stream [7, 8], catalytic combustion of hydrocarbons [9, 10], and selective hydrogenation [11, 12]. Supported Au nanoparticles possess unusually high activity for low-temperature oxidation of CO, whereas they did not demonstrate a favorable low-temperature behavior in other reactions such as oxidation of air pollutants yet. It is therefore of interest to explore their ability to remove other air contaminants.

Formaldehyde, emitted widely from furniture, decorative materials and consumer products, is one of the most dominant air pollutants in indoor environments [13, 14]. Long-term exposure to indoor air containing HCHO, even in very small amounts of the order of a few ppm, can cause adverse effects on human health [15]. Thus, great efforts have been made to eliminate HCHO to satisfy the stringent environmental regulations and to achieve better indoor air quality. Catalytic oxidation was recognized as the most promising technology for removal of HCHO [16–19]. However, the complete oxidation of HCHO can occur only at moderate temperatures over most of the reported catalysts [20–22]. To increase the operating temperatures an extra heating device is needed, that enhances an operating cost and makes reaction conditions more severe. Thus, this approach is not suitable for the control of indoor air pollution. Accordingly, elimination of HCHO at room temperature is highly desirable due to its environmentally friendly reaction conditions and energy saving [16, 18, 23]. However, the development of effective catalysts for HCHO oxidation at ambient temperature is still a challenge for investigators [18, 24].

Supported noble metals were demonstrated to be promising catalysts for the complete oxidation of HCHO at a low and even at ambient temperature [18]. Recently, several studies related to HCHO removal at a low temperature have been carried out using supported noble metal (Pt, Rh, Au and Pd) [13, 16, 18, 25]. Pt/TiO_2 was identified as the most active among noble metal catalysts supported on TiO_2 while Au/TiO_2 showed no activities for HCHO oxidation at room temperature [16, 25]. Li et al. [26] found that 0.73 wt % Au/FeO_x catalysts were inactive in HCHO oxidation at room temperature while the complete oxidation of HCHO can be obtained at 80°C when the Au content was increased to an a level as high as 7.1 wt %. In the literature, the

[1] The article is published in the original.

gold catalysts for HCHO oxidation were generally treated by calcinations in air at a high temperature [16, 22, 25, 26]. This treatment may lead to the agglomeration of gold nanoparticles especially in the presence of chloride ion [27]. In addition, the level of several hundred ppm of HCHO used for the performance test is much higher than the actual concentration of HCHO in indoor environments, which generally ranges from dozens of ppb to a ppm level. Therefore, it is of scientific and practical interest to attempt to study the room-temperature characteristics for low-concentrated HCHO oxidation over the supported Au catalysts.

The present work is aimed at extending the application of Au nanoparticles to removal of contaminants from air. It was also of interest to investigate the mechanism of conversion of HCHO. Highly active Au/TiO_2 catalysts were prepared by impregnation method followed by sodium borohydride reduction under mild conditions. Calcined Au nanoparticles were also prepared for comparison. They were used to study HCHO oxidation at room temperature. The catalysts were investigated by X-ray diffraction (**XRD**), BET surface area measurements, X-ray photoelectron spectroscopy (**XPS**) and transmission electron microscopy (**TEM**) techniques. An attempt was made to correlate the results of characterization of catalysts with their catalytic performance. Reduced Au/TiO_2 catalysts were successfully used to completely eliminate low concentrations of formaldehyde in air at room temperature.

EXPERIMENTAL SECTION

Catalyst Preparation

Both reduced and calcined Au/TiO_2 catalysts were prepared using TiO_2 powder (P25, "Degussa") as a support and $HAuCl_4$ as the precursor compound. The reduced Au/TiO_2 catalysts (denoted as Au/TiO_2-R) were prepared as follows. TiO_2 was uniformly dispersed into the $HAuCl_4$ solution. After impregnation for 1 h, $NaBH_4$ solution as reducing agent was quickly added into the suspension (molar ratio $NaBH_4 : Au = 10 : 1$) with vigorous stirring. After reduction, the suspension was dried at 80°C with continuous stirring. Finally, the samples were heated at 120°C in air for 4 h without further high temperature treatment. The calcined Au/TiO_2 catalyst (denoted as Au/TiO_2-C) was prepared as follows. TiO_2 was added into the $HAuCl_4$ solution with stirring. One hour later, the suspension was dried at 80°C with continuous stirring. The dried samples were further heated at 120°C for 4 h, followed by the calcination at 400°C in air for 4 h.

Catalyst Characterization

TEM images were recorded with a Tecnai G2 20 microscope operated at 200 kV. Surface areas were computed using the BET equations determined by measurements of N_2 adsorption–desorption isotherms at 77 K using a Micromeritics ASAP 2020 instrument. Prior to the measurements, the samples were degassed at 573 K for 2 h. XRD patterns were collected with a Bruker D8 Advance *X*-ray powder diffractometer, using CuK_α ($\lambda = 1.5418$ Å) radiation. The working voltage of the instrument was 40 kV and the current was 40 mA. The intensity data were collected in a 2θ range from 20° to 90°. XPS measurements of the catalysts were performed with a Physical Electronics 5600 multi-technique system using a monochromatic AlK_α source for the surface composition. The binding energy (**BE**) was determined by utilizing C1*s* line as a reference with energy of 285.0 eV.

Measurement of Catalytic Activity

The oxidation of HCHO was performed in a quartz tubular fixed-bed reactor with a 6 mm ID at atmospheric pressure and ambient temperature (25 ± 1°C). In a typical experiment 0.5 g of the catalyst (40–60 mesh) was loaded in the reactor. Gas-phase formaldehyde was obtained by bubbling the flow of zero air (only 21 vol % O_2 and 79 vol % N_2) through a saturator with HCHO solution. An air mixture containing 10 ppm HCHO, water vapor (50% relative humidity) was introduced as the reactant. The total flow rate was 1 L/min, corresponding to a gas hourly space velocity (**GHSV**) of 120000 mL g_{cat}^{-1} h^{-1}. The contents of HCHO and CO_2 in the air stream were ruonitored using an HCHO analyzer (Formaldemeter 400, "PPM Technology") and CO_2 analyzer (HAL-$HCO_2$01, "Chinaway Environmental Instruments"), respectively.

RESULTS AND DISCUSSION

Catalyst Characterization

Representative TEM micrographs for Au/TiO_2-R and Au/TiO_2-C (1 wt % Au) are presented in Fig. 1. Significant differences between the TEM micrographs of the Au/TiO_2-R sample and the thermally treated catalyst are evident. It can be seen that small Au nanoparticles of about 3.5 nm, uniformly distributed on the surface of the Au/TiO_2-R catalyst (Figs. 1b and 1c), become much larger on the Au/TiO_2-C catalyst (Fig. 1a). The gold nanoparticles are hardly discernable in the image of the 0.1%Au/TiO_2-R (Fig. 1d) catalyst due to a low gold content. Au particles prepared by the impregnation method are usually larger than 30 nm because the interaction of the Au precursors with the metal oxide support is weak, and chloride remaining on the support surfaces markedly promotes the coagulation of Au particles during calcination [27, 28]. However, mild preparation conditions for Au/TiO_2-R in this study can avoid significant Au sintering and conglobation, and favor the formation of uniform Au clusters with small size.

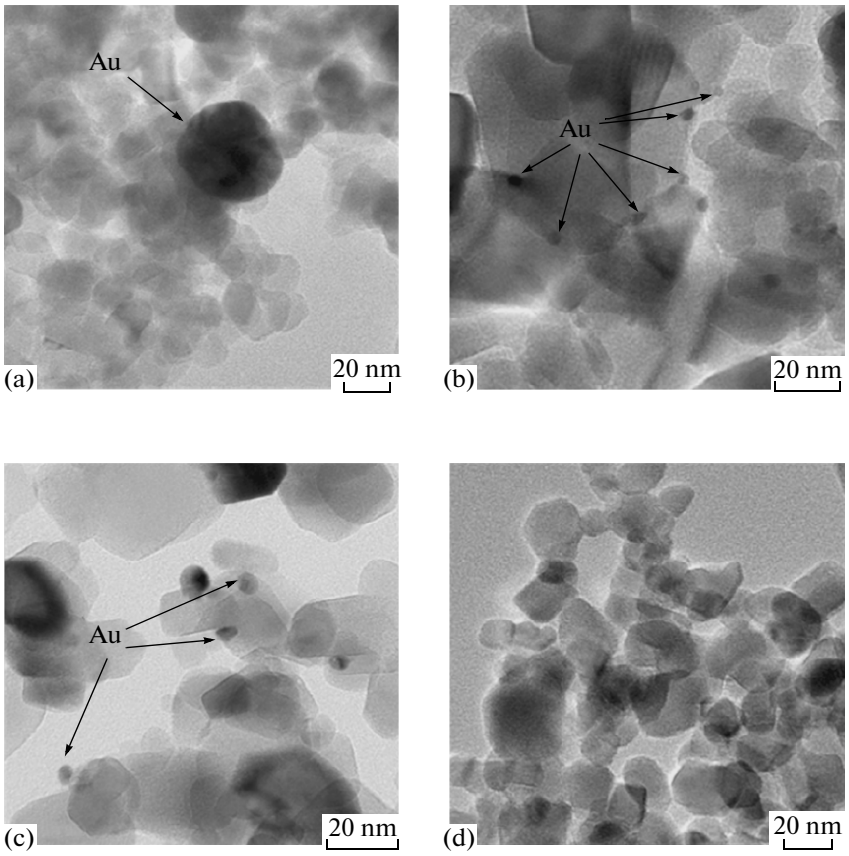

Fig. 1. *TEM* micrographs of Au catalysts: 1%Au/TiO_2-C (a), 1%Au/TiO_2-R (b), 0.5%Au/TiO_2-R (c) and 0.1%Au/TiO_2-R (d).

Table 1 summarizes the BET surface areas computed for Au/TiO_2 samples and for pure TiO_2. There are small differences in the surface area of the 1%Au/TiO_2-C catalyst and that of pure TiO_2. Nevertheless, while the 0.1 wt % Au/TiO_2-R catalyst shows nearly the same surface area as the pure TiO_2 the value of the surface area decreases with increasing Au content. The reason is that Au nanoparticles can cover the surface of TiO_2 and block its pores. As observed on the TEM images, many Au nanoparticles are highly dispersed in the Au/TiO_2-R catalyst, and that may cause the loss of the surface area [4]. Despite of the slight reduction in the BET surface area, the Au/TiO_2-R catalyst prepared by sodium borohydride reduction under mild reaction still preserves a well developed surface.

The crystallinity of pure TiO_2 and Au/TiO_2 was investigated using XRD measurements (Fig. 2). The XRD patterns of 1 wt % Au/TiO_2-R are essentially the same as that of pure TiO_2. In agreement with formerly reported results [26], Au peaks of the reduced catalyst were not significant, suggesting that Au nanoparticles are very small and highly dispersed on the support. In contrast, weak Au peaks were observed in the spectrum of the calcined sample, suggesting the presence of large Au nanoparticles which were also observed in the TEM micrographs (Fig. 1a). The peaks at $2\theta = 38.2°$ and 44.4° are attributed to (111) and (200) lattice planes of Au, respectively [26].

Catalytic Test

Figure 3 shows the time dependence of HCHO removal efficiency for the reduced and calcined catalysts Au/TiO_2 together with the data obtained for pure TiO_2 at ambient temperature. The oxidation of HCHO by pure TiO_2 can be excluded since no CO_2 was identified during the reaction. Removal of HCHO in the presence of pure TiO_2, 1%Au/TiO_2-C and

Table 1. BET surface areas of Au/TiO_2 catalysts and pure TiO_2

Sample	S_{BET}, m^2/g
TiO_2	50.8
0.1%Au/TiO_2-R	50.3
0.5%Au/TiO_2-R	45.7
1%Au/TiO_2-R	44.1
1%Au/TiO_2-C	50.6

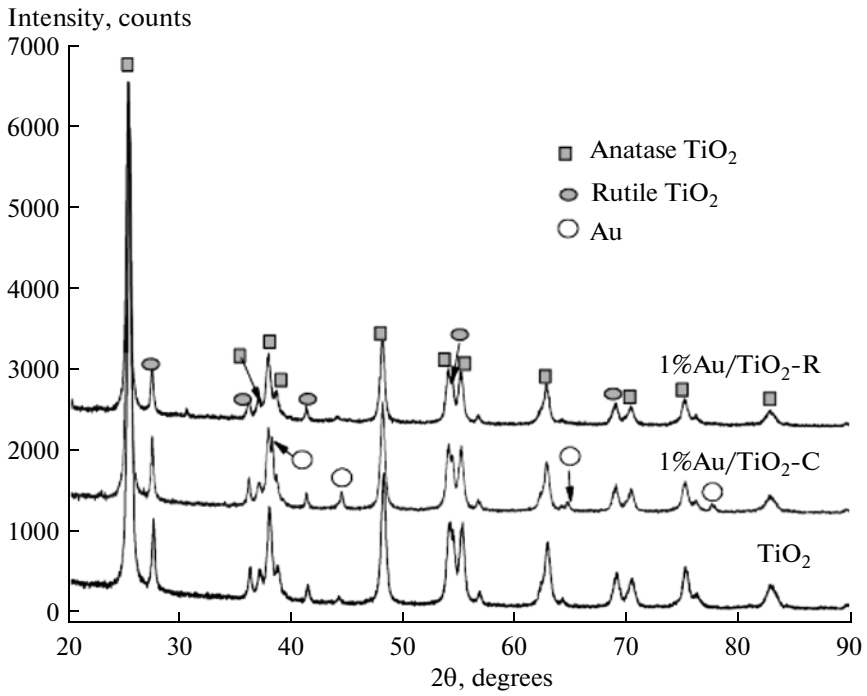

Fig. 2. XRD patterns of TiO_2, 1%Au/TiO_2-C and 1%Au/TiO_2-R.

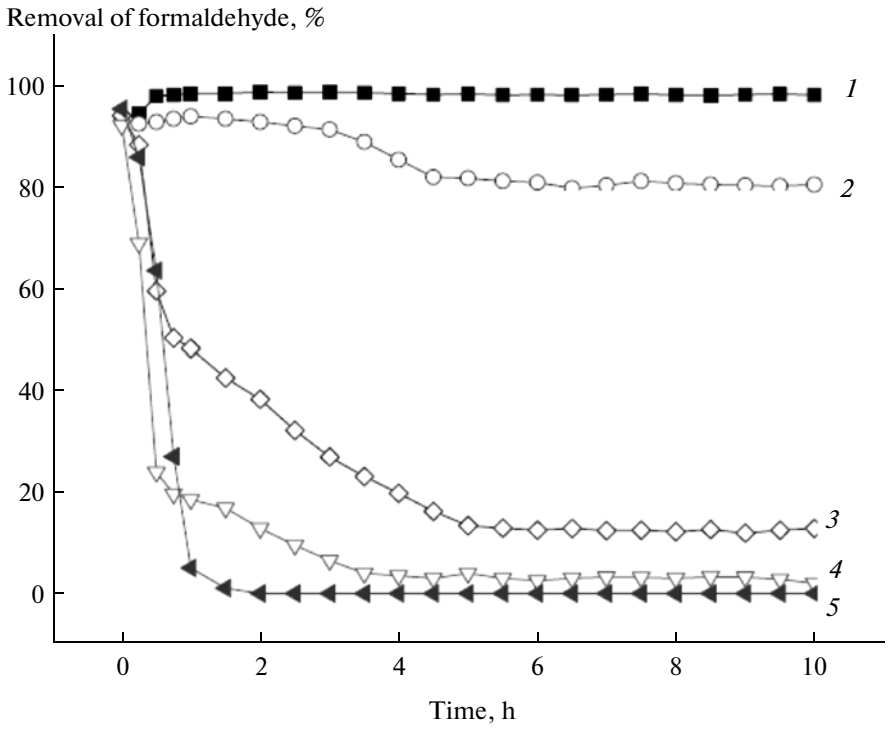

Fig. 3. The efficiency of HCHO removal for 1%Au/TiO_2-R (*1*), 0.5%Au/TiO_2-R (*2*), 0.1%Au/TiO_2-R (*3*), 1%Au/TiO_2-C (*4*) and pure TiO_2 (*5*).

0.1%Au/TiO_2-R at the initial stage was mainly ascribed to adsorption of the pollutant gas by TiO_2. The results show that the activities of catalysts were greatly influenced by the catalyst preparation methods. When compared with 1%Au/TiO_2-C, the Au/TiO_2-R catalyst shows an improved efficiency to

Table 2. XPS data for 1 wt % Au/TiO_2 catalysts

Catalyst	BE, eV				Surface atomic ratio O_{II}/O_I	Surface content, wt %	
	$Au4f_{7/2}$	O_{II}	O_I	$Ti2p$		Au	Cl
Au/TiO_2-C	84.9	532.2	530.6	459.8	0.075	0.23	0.25
Au/TiO_2-R	83	531.4	529.6	458.4	0.19	0.75	2.75

remove HCHO (Fig. 3). Only about 2.5% of HCHO was converted at the stationary stage over the 1%Au/TiO_2-C catalyst, whereas the conversion was remarkably increased to 98.5% over 1%Au/TiO_2-R. When the Au loading on the reduced catalysts was reduced to 0.5 and 0.1 wt %, the conversion of HCHO decreased respectively to 80.4 and 12.3%. It is understandable that a high Au loading provides additional active sites for HCHO oxidation, thus leading to higher HCHO conversions.

The most important factors controlling the catalytic activity of Au catalyst appear to be the particle size, the nature of a support and the oxidation state of Au [29]. It is well known that dispersion and particle size of noble metal nanoparticles are crucial factors for catalytic activity. The smaller the size of nanoparticles the higher the number of active surface atom and active center formed on the catalyst surface, and a better catalytic activity [22]. As observed in the TEM images, highly dispersed metallic Au nanoparticles with mean size of about 3.5 nm were formed in the Au/TiO_2-R catalyst. In spite of the fact that the average size of Au nanoparticles is similar for 1%Au/TiO_2-R and 0.5%Au/TiO_2-R catalyst, the former catalyst shows a higher HCHO conversion than the latter. This phenomenon can be explained by a higher mobility of lattice oxygen in the 1%Au/TiO_2-R catalyst.

The residual chlorine was identified in both 1%Au/TiO_2-C and Au/TiO_2-R by XPS. The surface chlorine concentration in the 1%Au/TiO_2-R catalyst (2.75 wt %) is much larger than that in the 1%Au/TiO_2-C sample (0.25 wt %) (Table 2), indicating that some chlorine was removed from 1%Au/TiO_2-C during calcinations while a considerable amount of chlorine was accumulated on the surface of the catalyst after $NaBH_4$ reduction. On the contrary, much higher conversions of HCHO were observed in the presence of the 1%Au/TiO_2-R catalyst than with the calcined sample. Highly efficient Au/TiO_2 catalysts for this reaction can be prepared in a very simple process and the dechlorination is not imperative.

The oxidation state of Au species was also important for CO oxidation [30, 31]. Some authors believe that ionic Au provides the active sites for CO oxidation [32, 33], others claimed metallic Au to be the active species [1, 30, 34]. The XPS analysis was carried out to identify the oxidation states of Au particles. XPS spectra of the Au4*f* are shown in Fig. 4a. It can be observed that the Au4*f* peak for 1%Au/TiO_2-C was centered at 84.9 eV, this energy is higher than that of Au^0, but lower than those of Au^+ and Au^{3+}. These results suggest the existence of gold species in a transition state between metallic and cationic gold. It is reported that $Au4f_{7/2}$ peaks of Au^0 (e.g. Au), Au^+ (e.g. AuCl) and Au^{3+} (e.g. $NaAuCl_4$) are centered at 83.8, 86.1 and 87.3 eV, respectively [3, 35]. Calcination at high temperature resulted in partial reduction of cationic Au to metal. In the case of the reduced Au catalyst, the peaks of $Au4f_{7/2}$ and $Au4f_{5/2}$ are centered at 83 and 86.65 eV ($\Delta = 3.65$ eV), suggesting that Au nanoparticles are fully reduced into metallic state [30, 36]. Interestingly, the $Au4f_{7/2}$ showed a significant negative shift of 1 eV for Au/TiO_2-R, with respect to that of bulk metallic Au (84.0 eV), indicating a very strong interaction between Au particles and the support. A strong metal–support interaction (SMSI) was confirmed by the BE shifts of O1*s* and Ti2*p*.The main peaks of O1*s* and $Ti2p_{3/2}$ on 1 wt % Au/TiO_2-C are located at 530.6 and 459.8 eV, respectively, which are close to values characteristic of lattice oxygen and Ti^{4+} in TiO_2 [37]. In comparison, the corresponding O and Ti peaks on 1%Au/TiO_2-R made a significant negative shift of 1 and 1.4 eV. The strong metal–support interaction can influence the electronic properties of the surface Au [38]. It was proposed that electron transfer from TiO_2 to Au core should be responsible for the shift of Au4*f* BE [30, 36, 39]. It is reasonable to suggest that electron transfer from the TiO_2 support to Au particles is facilitated due to a large difference in the work function between Au (5.27 eV) and TiO_2 (4.1 eV). This effect can be more pronounced for smaller Au particles due to the reduced coordination number of surface Au atoms [40]. The charge transfer was also proved by the notable BE shift of Ti2*p* of 1%Au/TiO_2-R. As shown in Fig. 4c, $Ti2p_{3/2}$ peak of 1%Au/TiO_2-R was shifted to a lower energy in comparison with the calcined sample, suggesting that Ti^{4+} is reduced into a lower valence and exists as TiO_x ($x < 2$). Oxygen vacancies on TiO_x play an important role in anchoring the Au particles and in transferring electron to Au [41]. In this way they facilitate adsorption of oxygen at the perimeter of Au particles. Negatively charged Au clusters also show

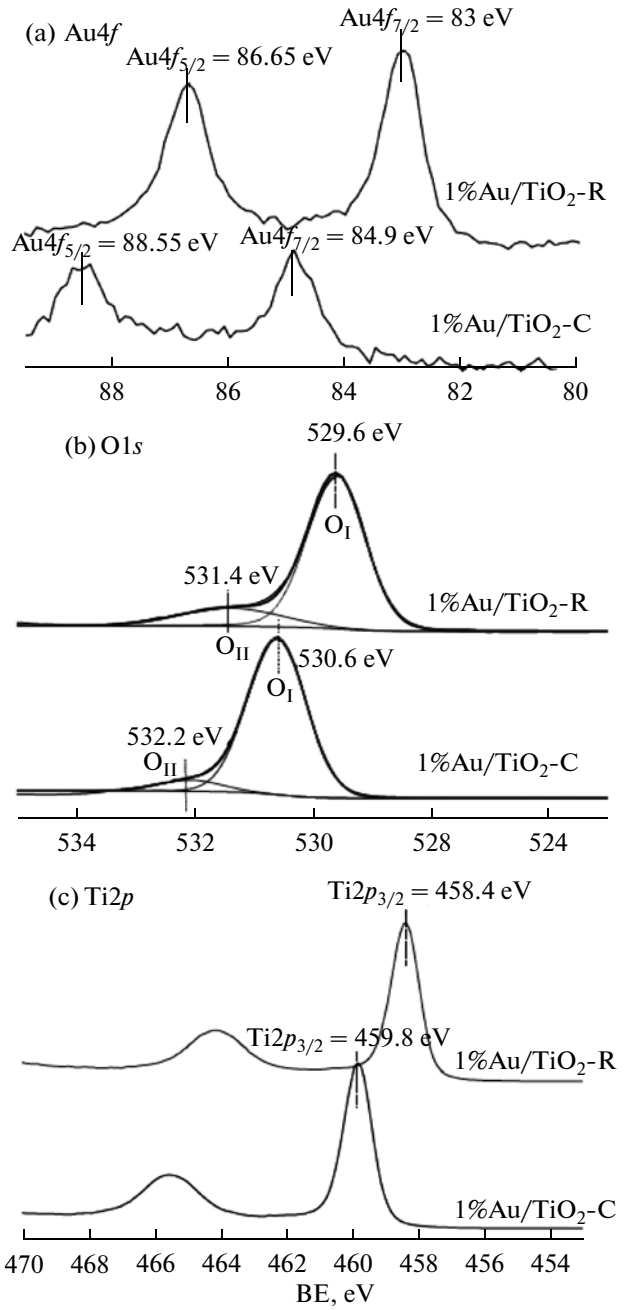

Fig. 4. *XPS* spectra of 1 wt % Au/TiO_2-R and Au/TiO_2-C: a—Au4*f*, b—O1*s*, c—Ti2*p*.

enhanced O_2 adsorption since the donation from the metal to the anti-bonding π* orbital of O_2 is enhanced [30, 42]. Charge transfer from Au nanoparticles to oxygen activates the oxygen molecule [43]. It was postulated that the activated oxygen exists in the form of Au–O complexes on the Au catalyst [34]. It is highly active and could easily exchange with the oxygen in the gas or in the molecules adsorbed on the catalysts [44, 45]. Negatively charged Au nanoparticles and oxygen vacancies generated by the reduction of supports can facilitate the electron transfer and contribute to the activation of oxygen and delivery of oxygen to the sites active in oxidation. This can explain why nano-sized Au particles deposited on reducible support, such as TiO_2 and CeO_2, show an increased activity for CO oxidation compared to gold particles on non-reducible support such as SiO_2 and Al_2O_3 [46].

The presence of activated oxygen was confirmed by XPS spectra of O1*s*. In Fig. 4b XPS spectra of 1%Au/TiO_2-R are compared with those of 1%Au/TiO_2-C. It can be seen that O1*s* spectra of Au/TiO_2-R exhibit two strong peaks: a main peak at 529.6 eV (denoted as O_I) and a shoulder at 531.4 eV (denoted as O_{II}). These results indicate that two types of oxygen exist on the surface of the Au/TiO_2 catalyst. The peak due to O_I can be attributed to the lattice oxygen of TiO_2 [44, 47–49]. The peak of O_{II} can represent an active state of oxygen, which possesses a high mobility and might be deeply involved in the redox cycles of HCHO oxidation. It can be proposed that O_{II} is attributable to chemisorbed oxygen in the form of Au–O complexes on the surface of Au catalyst. XPS spectra of O1*s* agree well with the observed XANES spectra observed over a fully reduced Au/TiO_2 catalyst in the previous reports [34, 43]. It can also be found that O_{II} peak of the 1%Au/TiO_2-R catalyst is much stronger than that of the 1%Au/TiO_2-C sample. As shown in Table 2 and Fig. 4b, the O_{II}/O_I ratio of 0.19 calculated from the deconvoluted peak observed for the 1%Au/TiO_2-R sample, is significantly higher than the ratio of 0.075 found for the calcined sample. A larger content of O_{II} atoms accounts for a higher HCHO conversion over 1%Au/TiO_2-C as evidenced by results of the catalytic activity test (Fig. 3). It can be concluded that the 1%Au/TiO_2-R catalyst is superior to the calcined sample in terms of the ability to activate O_2 and form the surface oxygen.

As shown in Table 2, the surface concentration of Au on Au/TiO_2-C is only 0.23%, which is apparently smaller than a bulk loading of the 1 wt % Au. This indicates that Au species predominantly occupy positions in the inner pores of the support of the calcined catalyst and that causes a decreased surface concentration of Au species [38]. However, as shown in Table 2, the surface concentration of Au in the reduced catalyst increases to 0.75%. A higher content of Au nanoparticles on the surface of TiO_2 facilitates a contact of the gold with HCHO molecule from the feed stream. The enrichment of Au particle on the surface leads to a higher concentration of active sites and to a larger amount of activated oxygen involved in the oxidation of HCHO. These factors account for a much higher activity of the 1%Au/TiO_2-R catalyst compared with the 1%Au/TiO_2-C sample.

The changes in textural properties of Au/TiO_2 are related to the aggregation state of Au. As described above, BET surface area of the calcined catalyst remained nearly the same as that of pure TiO_2 while it is reduced to 44.1 m^2/g for the 1%Au/TiO_2-R catalyst. An increased surface concentration of Au is appar-

ently responsible for a decrease in the BET surface area. It seems that Au nanoparticles attached to the surface of TiO_2 can block the adsorption sites of TiO_2. The highest HCHO conversion was obtained over 1%Au/TiO_2-R with the lowest BET surface area, suggesting that the oxidation of HCHO is not sensitive the values of the BET surface area.

The account given in this work indicates that Au/TiO_2 catalysts, prepared by sodium borohydride reduction, can be successfully used to completely eliminate low-concentrated formaldehyde in air at room temperature. The 1 wt % Au/TiO_2-R catalyst was found to be highly efficient for the oxidation of low-concentrated formaldehyde at room temperature. In the presence of this catalyst a 98.5% conversion of HCHO was achieved whereas the Au/TiO_2-C sample was nearly inactive under the same conditions. Highly dispersed metallic Au nanoparticles with a small average size (~3.5 nm) were identified in the 1 wt % Au/TiO_2-R catalyst. A significant negative shift of Au4*f* peak with respect to bulk metallic Au was observed for the 1 wt % Au/TiO_2-R catalyst but no similar phenomena was found for the calcined sample. More Au nanoparticles and a higher content of active oxygen were identified on the surface of the Au/TiO_2-R compared to the Au/TiO_2-C sample. The treatment by sodium borohydride reduction is favorable for the formation of finely dispersed metallic Au nanoparticles with small size. These particles facilitate the electron transfer, and increase the content of surface Au nanoparticles and activated oxygen. And these factors contribute to the high catalytic activity of Au catalysts in the oxidation of HCHO.

ACKNOWLEDGMENTS

The authors gratefully acknowledge the financial supports from the CRCG of the University of Hong Kong (Grant no. 200907176159).

REFERENCES

1. Haruta, M., Yamada, N., Kobayashi, T., and Iijima, S., *J. Catal.*, 1989, vol. 115, p. 301.
2. Herzing, A.A., Kiely, C.J., Carley, A.F., Landon, P., and Hutchings, G.J., *Science*, 2008, vol. 321, p. 1331.
3. Wang, D., Hao, Z., Cheng, D., Shi, X., and Hu, C., *J. Mol. Catal. A: Chem.*, 2003, vol. 200, p. 229.
4. Schwartz, V., Mullins, D.R., Yan, W., Chen, B., Dai, S., and Overbury, S.H., *J. Phys. Chem. B*, 2004, vol. 108, p. 15782.
5. Seker, E. and Gulari, E., *Appl. Catal., A*, 2002, vol. 232, p. 203.
6. Nguyen, L.Q., Salim, C., and Hinode, H., *Appl. Catal., A*, 2008, vol. 347, p. 94.
7. Sangeetha, P. and Chen, Y.-W., *Int. J. Hydrogen Energy*, 2009, vol. 34, p. 7342.
8. Luengnaruemitchai, A., Osuwan, S., and Gulari, E., *Int. J. Hydrogen Energy*, 2004, vol. 29, p. 429.
9. Haruta, M., Ueda, A., Tsubota, S., and Torres Sanchez, R.M., *Catal. Today*, 1996, vol. 29, p. 443.
10. Scir, S., Minic, S., Crisafulli, C., Satriano, C., and Pistone, A., *Appl. Catal., B*, 2003, vol. 40, p. 43.
11. Cardenas-Lizana, F., de Pedro, Z.M., Gomez-Quero, S., and Keane, M.A., *J. Mol. Catal. A: Chem.*, 2010, vol. 326, p. 48.
12. Nikolaev, S.A. and Smirnov, V.V., *Catal. Today*, 2009, vol. 147, p. 336.
13. Wang, L., Sakurai, M., and Kameyama, H., *J. Hazard. Mater.*, 2009, vol. 167, p. 399.
14. Peng, J.X. and Wang, S.D., *Appl. Catal., B,* 2007, vol. 73, p. 282.
15. Sekine, Y., *Atmos. Environ.*, 2002, vol. 36, p. 5543.
16. Zhang, C.B., He, H., and Tanaka, K., *Appl. Catal., B*, 2006, vol. 65, p. 37.
17. He, Y.B. and Ji, H.B., *Chin. J. Catal.*, 2010, vol. 31, p. 171.
18. Tang, X.F., Chen, J.L., Huang, X.M., Xu, Y., and Shen, W.J., *Appl. Catal., B*, 2008, vol. 81, p. 115.
19. Peng, J. and Wang, S., *J. Phys. Chem. C,* 2007, vol. 111, p. 9897.
20. Alvarez-Galvan, M.C., Pawelec, B., de la Pena, O., Shea, V.A., Fierro, J.L.G., and Arias, P.L., *Appl. Catal., B*, 2004, vol. 51, p. 83.
21. Tang, X.F., Li, Y.G., Huang, X.M., Xu, Y.D., Zhu, H.Q., Wang, J.G., and Shen, W.J., *Appl. Catal., B*, 2006, vol. 62, p. 265.
22. Shen, Y., Yang, X., Wang, Y., Zhang, Y., Zhu, H., Gao, L., and Jia, M., *Appl. Catal., B*, 2008, vol. 79, p. 142.
23. Wang, L.F., Zhang, Q., Sakurai, M., and Kameyama, H., *Catal. Commun.*, 2007, vol. 8, p. 2171.
24. Zhang, C.B., He, H., and Tanaka, K., *Catal. Commun.*, 2005, vol. 6, p. 211.
25. Zhang, C. and He, H., *Catal. Today*, 2007, vol. 126, p. 345.
26. Li, C., Shen, Y., Jia, M., Sheng, S., Adebajo, M.O., and Zhu, H., *Catal. Commun.*, 2008, vol. 9, p. 355.
27. Kung, H.H., Kung, M.C., and Costello, C.K., *J. Catal.*, 2003, vol. 216, p. 425.
28. Haruta, M., *CATTECH*, 2002, vol. 6, p. 102.
29. Kung, M.C., Davis, R.J., and Kung, H.H., *J. Phys. Chem. C*, 2007, vol. 111, p. 11767.
30. Arrii, S., Morfin, F., Renouprez, A.J., and Rousset, J.L., *J. Am. Chem. Soc.*, 2004, vol. 126, p. 1199.
31. Grisel, R.J.H. and Nieuwenhuys, B.E., *Catal. Today*, 2001, vol. 64, p. 69.
32. Park, E. and Lee, J., *J. Catal.*, 1999, vol. 186, p. 1.
33. Fu, Q., Saltsburg, H., and Flytzani-Stephanopoulos, M., *Science,* 2003, vol. 301, p. 935.
34. Weiher, N., Beesley, A.M., Tsapatsaris, N., Delannoy, L., Louis, C., van Bokhoven, J.A., and Schroeder, S.L.M., *J. Am. Chem. Soc.*, 2007, vol. 129, p. 2240.
35. Ribeiro, N.F.P., Mendes, F.M.T., Perez, C.A.C., Souza, M.M.V.M., and Schmal, M., *Appl. Catal., A,* 2008, vol. 347, p. 62.
36. Chen, Y., Zhu, B., Yao, M., Wang, S., and Zhang, S., *Catal. Commun.*, 2010, vol. 11, p. 1003.

37. Chen, X. and Burda, C., *J. Phys. Chem. B*, 2004, vol. 108, p. 15446.
38. Huang, J., Dai, W.-L., Li, H., and Fan, K., *J. Catal.*, 2007, vol. 252, p. 69.
39. Yu, K., Wu, Z., Zhao, Q., Li, B., and Xie, Y., *J. Phys. Chem. C*, 2008, vol. 112, p. 2244.
40. Fu, P. and Zhang, P., *Appl. Catal., B*, 2010, vol. 96, p. 176.
41. Chen, M. and Goodman, D.W., *Acc. Chem. Res.,* 2006, vol. 39, p. 739.
42. Hutchings, G.J., *Dalton Trans.*, 2008, vol. 7, p. 5523.
43. Van Bokhoven, J.A., Louis, C., Miller, J.T., Tromp, M., Safonova, O.V., and Glatzel, P., *Angew. Chem. Int. Ed.*, 2006, vol. 45, p. 4651.
44. Yang, S., Feng, Y., Wan, J., Zhu, W., and Jiang, Z., *Appl. Surf. Sci.*, 2005, vol. 246, p. 222.
45. Gabasch, H., Knop-Gericke, A., Schlegl, R., Borasio, M., Weilach, C., Rupprechter, G., Penner, S., Jenewein, B., Hayek, K., and Kletzer, B., *Phys. Chem. Chem. Phys.*, 2007, vol. 9, p. 533.
46. Delannoy, L., Weiher, N., Tsapatsaris, N., Beesley, A., Nchari, L., Schroeder, S., and Louis, C., *Top. Catal.,* 2007, vol. 44, p. 263.
47. Yang, S., Zhu, W., Jiang, Z., Chen, Z., and Wang, J., *Appl. Surf. Sci.*, 2006, vol. 252, p. 8499.
48. Wu, Z., Sheng, Z., Liu, Y., Wang, H., Tang, N., and Wang, J., *J. Hazard. Mater.*, 2009, vol. 164, p. 542.
49. Min, B.K., Wallace, W.T., and Goodman, D.W., *J. Phys. Chem. B*, 2004, vol. 108, p. 14609.